THE GEOLOGICAL SOCIETY OF AMERICA®

The origin of contractional structures in extensional gneiss domes

P.F. Rey[1], L. Mondy[1], G. Duclaux[2], C. Teyssier[3], D.L. Whitney[3], M. Bocher[4], and C. Prigent [5]
[1]School of Geosciences, University of Sydney, Sydney, NSW 2006, Australia
[2]Department of Earth Science, University of Bergen, Bergen 5007, Norway
[3]Department of Earth Sciences, University of Minnesota, Minneapolis, Minnesota 55455, USA
[4]Laboratoire de Géologie de Lyon, Université Claude Bernard, Lyon 1, F-69622 Villeurbanne, France, and Ecole Normale Supérieure de Lyon, F-69342 Lyon, France
[5]Université Grenoble Alpes, CNRS, ISTerre, F-38000 Grenoble, France

ABSTRACT

The juxtaposition of domains of shortening and extension at different scales in orogens has fueled many debates about driving forces and tectonic interpretations, including timing of deformation. At the orogen scale, gravitational collapse and mass transfer from orogenic plateaux to forelands explain some of these juxtapositions. At a regional scale, structures in gneiss domes are commonly contractional yet are coeval with regional extension and denudation. Here we use three-dimensional numerical experiments to show that crustal flow in orogenic domains does not necessarily conform to plate motion. We document contractional crustal flow associated with the formation of a gneiss dome in an orogenic pull-apart setting where localized extension and crustal thinning focus the exhumation of deep crust. We show that the flow field results in a complex strain pattern in which an extensional strain regime that is collinear with the direction of plate motion is partitioned into the shallow crust, whereas contractional structures and fabrics at a high angle to the direction of imposed transport develop in the deep crust. Advective mass transfer across regions of contrasting yet coeval strain regimes leads to a polyphase tectonic history. We observe structural features remarkably similar to those documented in some natural gneiss domes such as the Montagne Noire, which developed in a dextral pull-apart domain at the southern margin of the French Massif Central.

INTRODUCTION

In the 1980s, gravitational collapse of orogenic crust was proposed to explain regions of surface extension in zones of active convergence (Molnar and Chen, 1982; Coney and Harms, 1984; Dewey, 1988; England and Houseman, 1989). Under warm crustal conditions (i.e., Moho temperature, T_{Moho} > ~700 °C), superposition of the tectonic far-field stress related to displacement of neighboring plates and the gravitational stress generated by lateral variations in gravitational potential energy can lead to contrasting strain regimes in orogenic plateau and adjacent foreland regions (e.g., Sonder et al., 1987; Jones et al., 1996; England and Houseman, 1989; England and Molnar, 1997; Flesch et al., 2000; Rey et al., 2010). Strong vertical strain partitioning also develops during heterogeneous thinning of the upper crust, as convergent flow forces the ductile lower crust into gneiss domes in which contractional strain dominates while boundary-driven extension develops in the shallow crust (e. g. Wdowinski and Axen, 1992; Axen et al., 1998; Mancktelow and Pavlis, 1994; Rey et al., 2011; Le Pourhiet et al., 2012; Whitney et al., 2013; Molnar, 2015). Hence, gneiss domes represent prime targets to document and understand complex three-dimensional (3-D) flow through time.

Here, we simulate a dextral pull-apart basin through a set of 3-D coupled thermal-mechanical experiments that document complex flow and strain patterns. The pull-apart basin geometry is a simple 3-D setting capable of partitioning deformation between the brittle upper crust and the ductile lower crust, as well as horizontally across various domains where simple shear, extension, or contraction dominate. In the upper crust, we observe divergence and rigid translation collinear to the imposed kinematic conditions that are applied at the margin of the model. In contrast, flow of the warm ductile crust involves a curvilinear convergent motion toward the zone of pull-apart basin extension in the upper crust. Consequently, extension in the upper crust is coeval with contractional structures and fabrics in the lower crust. We compare the resulting structures to that of the Montagne Noire, a gneiss dome formed in a dextral pull-apart basin domain at the southern edge of the French Massif Central (Variscan orogen).

EXPERIMENTAL SETUP AND NUMERICAL METHODS

A block of continental lithosphere with dimensions 256 × 256 × 128 km is mapped over a computational mesh consisting of 192 × 192 × 96 elements (Fig. 1). The model includes, from top to bottom, an 8-km-thick layer of compressible air-like material, a layer of continental crust (40 km or 60 km thick), and a layer of mantle. Two non-overlapping, parallel and vertical faults are embedded into the upper part of the continental crust

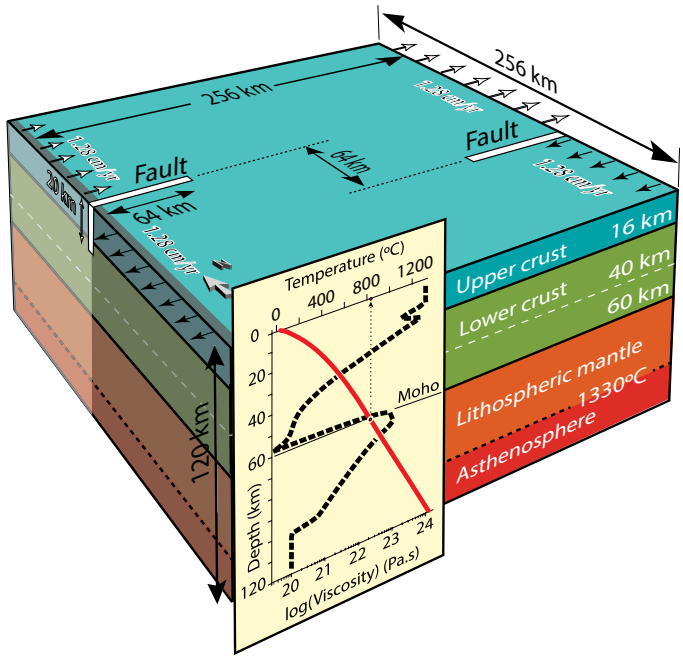

Figure 1. Experimental setup. Kinematic boundary conditions are applied on two opposite vertical walls via inflow and outflow of material driving overall dextral motion, opposite lithospheric blocks moving laterally at velocity of 1.28 cm yr^{-1} (i.e., total relative velocity of 2.56 cm yr^{-1}). Graph in front of model shows geotherm (solid curve) and viscosity profile (dashed curve) at time t = 0 yr.

Data Repository item 2017068 | doi:10.1130/G38595.1

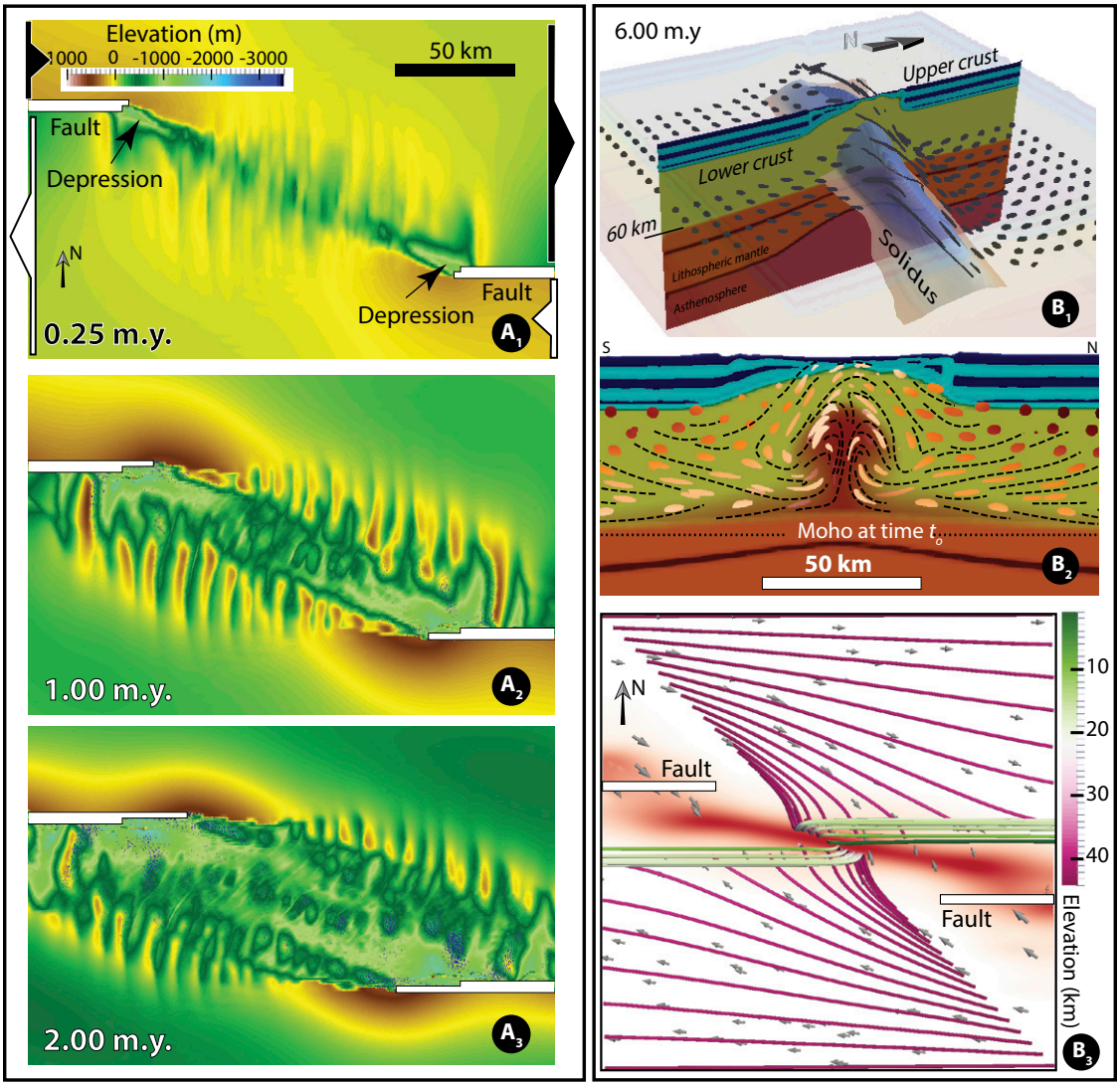

Figure 2. Strain fields for decoupled experiment. A: Maps of topographic surface showing evolution of deformation through time. B: Ductile strain field and flow field at 6 m.y. B_1: Three-dimensional view showing location of cross-section in panel B_2. Blue envelope shows solidus colored for temperature (blue is cold). Strain markers, initially spherical, are in dark gray. They were initially located at ~42 km depth before exhumation into upper crust (see also Fig. DR4 [see footnote 1]). B_2: Cross-section showing deformed strain markers in lower crust (hue varies with increased finite strain) and foliation trajectories (dashed lines). Red shading in lower crust shows melt fraction up to maximum of 18%. B_3: Streamlines colored for elevation starting at 44 km depth on horizontal northwest-southeast diagonal. They are aligned with direction of plate motion in shallow crust. Grey arrows show velocity vectors at 44 km depth.

(Fig. 1). The faults, made of material of weaker rheology (Table DR1 in the GSA Data Repository[1]), extend from the surface to 20 km depth and laterally over a distance of 64 km from the two opposite vertical walls. Kinematic boundary conditions drive divergence at a total velocity of 2.56 cm yr^{-1} (Fig. 1) promoting the formation of a pull-apart basin.

The density of all rocks varies with temperature and melt fraction when temperature $T > T_{solidus}$ (Fig. 1; Table DR1). The rheology of crust and mantle follows a visco-plastic formulation, which incorporates a strain-weakening term (see the Data Repository and Table DR1) and a term taking into account the presence of partial melt (e.g., Rey and Müller, 2010). The geotherm derives from imposing radiogenic heat production in the crust, mantle heat flow at the base of the model (20 mW m^{-2}), and constant temperature in the uppermost air-like layer (20 °C). At the base of the model, the asthenosphere is allowed to flow in or out of the model to maintain a constant basal lithostatic pressure. A free slip boundary condition is imposed on the front and back vertical walls, and outflow or inflow on the left and right walls.

The open-source code Underworld (Moresi et al., 2003, 2007) solves the Stokes equation for a very low Reynolds number on a fixed regular Cartesian grid. Lagrangian particles (~212×10^6 in total) carrying material properties are advected through the grid at the nodes of which pressure and velocity are solved. We explore two contrasting settings in which the mantle is either mechanically coupled to, or decoupled from, the upper crust. Keeping the same initial temperature field for both sets of experiments, coupling or decoupling is achieved by considering a crust of normal thickness (i.e., 40 km, T_{Moho} ~630ºC) or a thicker crust (60 km, T_{Moho} ~830ºC). The lower section of the thicker crust is therefore warmer and weaker, which results in decoupling the strong upper crust from the strong lithospheric mantle.

RESULTS

In both coupled and decoupled experiments, the early stage of deformation is characterized by the development of a set of en échelon extensional fractures (Figs. 2A1–$2A_3$; Fig. DR1 and Figs. DR$2A_1$–$2A_3$ in the Data Repository) perpendicular to the direction of regional divergence. The resulting damaged zone helps focus deformation in the region limited by the two master faults (i.e., step-over region). At the tip of each master fault, a depression develops bounded by a set of conjugate normal faults. As extension proceeds, the two sets of conjugate normal faults and associated depressions propagate toward the center of the step-over region to form a pull-apart basin (Fig. 2A). Extension progressively focuses in the central depression where thinning of the brittle upper crust via normal faulting controls the flow of lower crust toward the pull-apart region (Fig. 2B).

[1]GSA Data Repository item 2017068, Underworld input scripts, detailed information and Table DR1 on numerical experiment parameters, and additional figures relevant to the model where the upper crust is coupled to the upper mantle, is available online at www.geosociety.org/datarepository/2017 or on request from editing@geosociety.org.

A cross-section perpendicular to the central depression (Figs. 2B$_1$–2B$_2$) reveals a finite strain pattern in the ductile crust that depends on the mechanical coupling between the mantle and the upper crust. In the case of strong lower crust (40-km-thick crust), strain partitioning is moderate (Fig. DR2B$_2$). In the experiment with a 60-km-thick crust, the weak lower crust flows within a subhorizontal channel toward the region below the developing pull-apart basin (Figs. 2B$_1$–2B$_2$). The convergent, isostatically driven deep crustal flow mitigates crustal thinning, and the Moho remains more or less flat (Fig. 2B$_2$); this contrasts with the more prominent Moho exhumation in the coupled experiment (Figs. DR2B$_2$ and DR3A).

Below the pull-apart basin a gneiss dome develops, assisted by decompression melting (decreased viscosity) during ascent of flowing crust (Figs. 2B$_2$–2B$_3$). The long axis of the dome is aligned with the direction of the damaged zone in the upper crust. In the deep crust, the subhorizontal velocity streamlines curve clockwise, converging toward the region below the pull-apart basin, where they become sub-perpendicular to the direction of plate motion (Fig. 2B$_3$). As deep crust flows into the growing dome, the streamlines rotate upward before becoming subhorizontal upon reaching the base of the stronger shallow crust. Streamlines in the shallow crust remain horizontal and collinear with the direction of plate motion (Fig. 2B$_3$). In the mechanically coupled experiment, streamlines largely conform to the imposed velocity boundary condition (Figs. DR2B$_3$–DR2BC).

In the decoupled experiment (60-km-thick crust), strain markers reveal a strongly partitioned strain regime between the shallow and the deep crust (Fig. 2B$_2$). Extensional deformation with shallowly dipping foliation develops just below the brittle-ductile transition (Fig. 2B$_2$). In contrast, contractional structures with steeply dipping foliation in a high-strain planar zone separate two folds of foliation that develop in the ductile crust below the pull-apart basin where deep crustal rocks are exhumed (Figs. 2B$_2$, 3B). This double fold is wrapped by a broad domical foliation fold that is elongated in the direction joining the tips of the master faults at an angle to the imposed velocity direction. In the deep crust, away from the pull-apart region, the stretching lineation is perpendicular to the velocity direction imposed at the margins of the model (Fig. 3A1). This lineation rotates in the region underneath the pull-apart basin to become locally prominent (constrictional strain) and broadly aligned with the imposed velocity direction (Figs. 2B$_3$, 3A). This stretching lineation makes an angle with the direction of the overarching dome and, as a consequence, plunges in opposite directions on both of its flanks (Fig. 3A). These structural features are far less prominent when the upper crust is coupled to the upper mantle (Figs. DR2B$_2$ and DR3).

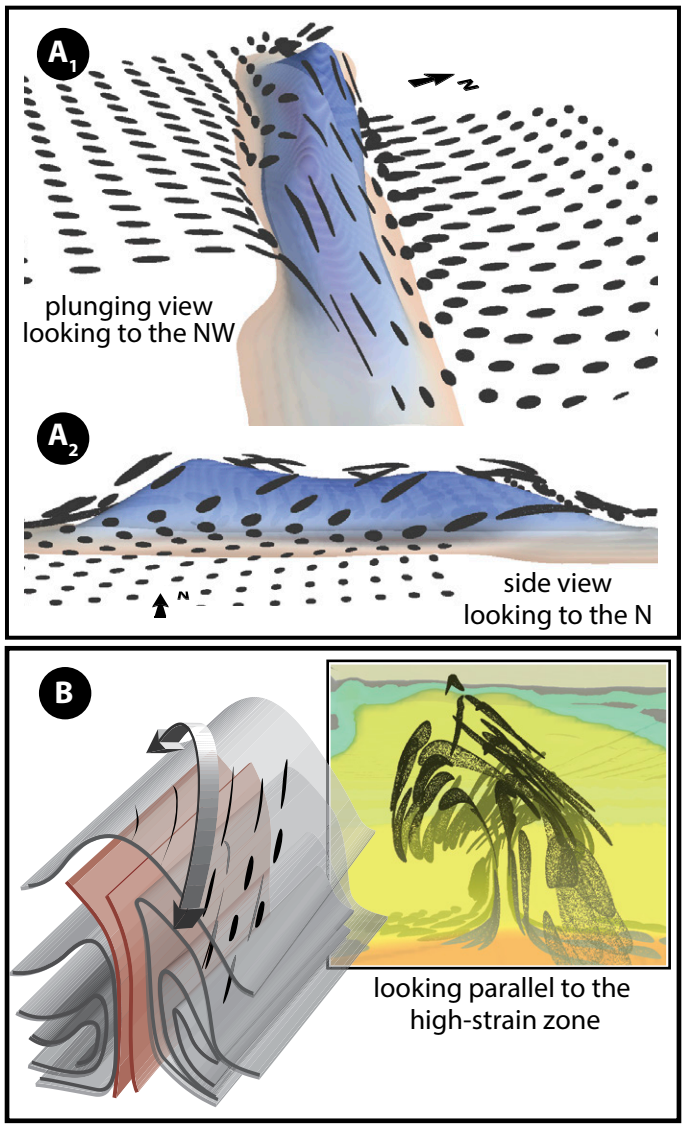

Figure 3. Internal structure and stretching lineation in decoupled experiment. A: Strain markers at 6 m.y. Markers were initially located at 42 km depth. B: Tectonogram illustrating double fold of foliation separated by high-strain zone (in red shading) underneath overarching foliation fold carrying stretching lineation curving over fold axis (black strain markers and curved arrows).

DISCUSSION

In the experiment in which the warm lower crust decouples the upper crust from the mantle, the finite strain field suggests a polyphase tectonic history. The early flat-lying, high-grade foliation and lineation (D1) are folded into two upright anticlinal folds (D2$_a$). The intervening syncline evolves into a high-strain zone (D2$_b$). These deep structures are exhumed underneath an extensional brittle-ductile detachment zone (D3$_a$) above which a set of normal faults (D3$_b$) accommodates thinning of the upper crust. Tectonic structures and fabrics are commonly directly related to tectonic regimes and therefore to plate motions or far-field boundary conditions. Accordingly, one may be tempted to conclude that a phase of convergence responsible for D2 structures preceded a phase of divergence resulting in D3 structures. However in our numerical experiments the far-field boundary conditions remain constant, and D1 to D3 structures develop at the same time but in different domains of contrasting yet coeval strain regimes. Importantly, the shallow part of the gneiss dome (<5 km depth) includes rocks exhumed from the base of the lower crust as shown by the passive strain markers (Fig. 2B; Fig. DR4). During their exhumation, these deep rocks traveled through contrasting strain domains where they potentially recorded D1 through D3 flattening to constrictional fabrics.

The structures and metamorphic association described above (Figs. 2B$_2$ and 3B) is remarkably similar to that documented in the Montagne Noire gneiss dome, which was exhumed between two dextral strike-slip faults at the southern end of the French Massif Central (Echtler and Malavieille, 1990; Roger et al., 2015). Detailed regional structural maps (e.g., Rabin et al., 2015) show that the Montagne Noire consists of a double dome, with the Agout-Espinouse dome to the north and the Nore-Caroux dome to the south, separated by a steeply dipping high-strain zone (Rey et al., 2011). The regional stretching lineation, locally constrictional, is oriented northeast-southwest at an angle to the ENE-WSW orientation of the Montagne Noire dome. The lineation plunges northeastward at the northeastern end of the dome, and southwestward at the southwestern end. Crystallization of migmatite and granite was coeval with the formation of the dome and has been dated at 315–305 Ma (Roger et al., 2015). Eclogite dated at ca. 315 Ma was exhumed from ~1.4 GPa to shallow crustal levels in <10 m.y. (Whitney et al., 2015), consistent with our experiment results showing rapid, large-scale exhumation of the deep crust in domes (Fig.

DR4B). Our numerical experiments confirm that the main structures of the Montagne Noire are compatible with a double dome emplaced into a dextral pull-apart basin (e.g., Echtler and Malavieille, 1990; Demange, 1999; Doublier et al., 2015; Roger et al., 2015). Similar double-dome structures occur in other orogens (e.g., Naxos dome, Aegean Sea; Aston-Hopitalet dome, Pyrenees; Entia dome, Alice Springs orogen, Australia).

CONCLUSIONS

In orogenic crust, localized thinning of the upper crust forces convergent flow in the lower crust leading to the formation and denudation of a gneiss dome. The flow field follows a complex pattern that is not conforming with imposed far-field motions. Contractional structures in the core of the dome develop coevally with extensional structures in the shallow part of the dome. Our 3-D experiments explain the upright, double foliation folds (double dome) separated by a steeply dipping high-strain zone and the strong shallowly plunging stretching lineation oblique to the dome axis observed in the Montagne Noire gneiss dome. The advective transfer of deep crust across regions of contrasting yet coeval strain regimes results in a polyphase tectonic history that developed during steady far-field motion.

ACKNOWLEDGMENTS

We thank L. Le Pourhiet, K. Gessner, and an anonymous reviewer for their helpful reviews. Underworld code is provided by AuScope Ltd., funded under the Australian National Collaborative Research Infrastructure Strategy. Australia National Computational Infrastructure provided computational resource. This research was supported by Australian Research Council's ITRH project IH130200012. U.S. National Science Foundation grant EAR-1050020 to CT and DLW funded field work in the Montagne Noire. GD is supported by Research Council of Norway FRINATEK project 234153.

REFERENCES CITED

Axen, G., Selverstone, J., Byrne, T., and Fletcher, J.M., 1998, If the strong lower crust leads, will the weak crust follow?: GSA Today, v. 8, no. 12, p. 1–8.

Coney, P.J., and Harms, T.A., 1984, Cordilleran metamorphic core complexes: Cenozoic extensional relics of Mesozoic compression: Geology, v. 12, p. 550–554, doi:10.1130/0091-7613(1984)12<550:CMCCCE>2.0.CO;2.

Demange, M., 1999, Evolution tectonique de la Montagne Noire: Un modèle en transpression: Comptes Rendus de l'Académie des Sciences de Paris, Series IIA: Earth and Planetary Science, v. 329, p. 823–829, doi:10.1016/S1251-8050(00)88638-3.

Dewey, J.F., 1988, Extensional collapse of orogens: Tectonics, v. 7, p. 1123–1139, doi:10.1029/TC007i006p01123.

Doublier, M.P., Potel, S., and Wemmer, K., 2015, The tectono-metamorphic evolution of the very low-grade hangingwall constrains two-stage gneiss dome formation in the Montagne Noire example (southern France): Journal of Metamorphic Geology, v. 33, p. 71–89, doi:10.1111/jmg.12111.

Echtler, H., and Malavieille, J., 1990, Extensional tectonics, basement uplift and Stephano-Permian collapse basin in a late Variscan metamorphic core complex (Montagne Noire, southern Massif Central): Tectonophysics, v. 177, p. 125–138, doi:10.1016/0040-1951(90)90277-F.

England, P.C., and Houseman, G., 1989, Extension during continental convergence, with application to the Tibetan Plateau: Journal of Geophysical Research, v. 94, p. 17,561–17,579, doi:10.1029/JB094iB12p17561.

England, P.C., and Molnar, P., 1997, Active deformation of Asia: From kinematics to dynamics: Science, v. 278, p. 647–650, doi:10.1126/science.278.5338.647.

Flesch, L.M., Holt, W.E., Haines, A.J., and Bingming, S.-T., 2000, Dynamics of the Pacific–North American plate boundary in the western United States: Science, v. 287, p. 834–836, doi:10.1126/science.287.5454.834.

Jones, C.H., Unruh, J., and Sonder, L.J., 1996, The role of gravitational potential energy in active deformation in the southwestern United States: Nature, v. 381, p. 37–41, doi:10.1038/381037a0.

Le Pourhiet, L., Huet, B., May, D.A., Labrousse, L., and Jolivet, L., 2012, Kinematic interpretation of the 3D shapes of metamorphic core complexes: Geochemistry Geophysics Geosystems, v. 13, Q09002, doi:10.1029/2012GC004271.

Mancktelow, N.S., and Pavlis, T.L., 1994, Fold-fault relationships in low-angle detachment systems: Tectonics, v. 13, p. 668–685, doi:10.1029/93TC03489.

Molnar, P., 2015, Gravitational instability of mantle lithosphere and core complexes: Tectonics, v. 34, p. 478–487, doi:10.1002/2014TC003808.

Molnar, P., and Chen, W.P., 1982, Seismicity and mountain building, *in* Hsu, K. J. ed., Mountain Building Processes: New York, Academic Press, p. 41–57.

Moresi, L.N., Dufour, F., and Mühlhaus, H.B., 2003, A Lagrangian integration point finite element method for large deformation modelling of viscoelastic geomaterials: Journal of Computational Physics, v. 184, p. 476–497, doi:10.1016/S0021-9991(02)00031-1.

Moresi, L., Quenette, S., Lemiale, V., Meriaux, C., Appelbe, B., and Mühlhaus, H.B., 2007, Computational approaches to studying non-linear dynamics of the crust and mantle: Physics of the Earth and Planetary Interiors, v. 163, p. 69–82, doi:10.1016/j.pepi.2007.06.009.

Rabin, M., Trap, P., Carry, N., Fréville, K., Cenki-Tonk, B., Lobjoie, C., Goncalves, Ph., and Marquer, D., 2015, Strain partitioning along the anatectic front in the Variscan Montagne Noire massif (southern French Massif Central): Tectonics, v. 34, p. 1709–1735, doi:10.1002/2014TC003790.

Rey, P.F., and Müller, R.D., 2010, Fragmentation of active continental plate margins owing to the buoyancy of the mantle wedge: Nature Geoscience, v. 3, p. 257–261, doi:10.1038/ngeo825.

Rey, P.F., Teyssier, C., and Whitney, D.L., 2010, Limit of channel flow in orogenic plateaux: Lithosphere, v. 2, p. 328–332, doi:10.1130/L114.1.

Rey, P.F., Teyssier, C., Kruckenberg, S.C., and Whitney, D. L., 2011, Viscous collision in channel explains double domes in metamorphic core complexes: Geology, v. 39, p. 387–390, doi:10.1130/G31587.1.

Roger, F., Teyssier, C., Respaut, J.-P., Rey, P.F., Jolivet, M., Whitney, D.L., Paquette, J.-L., and Brunel, M., 2015, Timing of formation and exhumation of the Montagne Noire double dome, French Massif Central: Tectonophysics, v. 640–641, p. 53–69, doi:10.1016/j.tecto.2014.12.002.

Sonder, L., England, P.C., Wernicke, B.P., and Christiansen, R.L., 1987, A physical model for Cenozoic extension of western North America, *in* Coward, M.P., et al., eds., Continental Extensional Tectonics: Geological Society of London Special Publication 28, p. 187–201, doi:10.1144/GSL.SP.1987.028.01.14.

Wdowinski, S., and Axen, G.J., 1992, Isostatic rebound due to tectonic denudation: A viscous flow model of a layered lithosphere: Tectonics, v. 11, p. 303–315, doi:10.1029/91TC02341.

Whitney, D.L., Teyssier, C., Rey, P.F., and Buck, W.R., 2013, Continental and oceanic core complexes: Geological Society of America Bulletin, v. 125, p. 273–298, doi:10.1130/B30754.1.

Whitney, D.L., Roger, F., Teyssier, C., Rey, P.F., and Respaut, J.-P., 2015, Syn-collapse eclogite metamorphism and exhumation of the deep crust in a migmatite dome: The P-T-t record of the youngest Variscan eclogite (Montagne Noire, French Massif Central): Earth and Planetary Science Letters, v. 430, p. 224–234, doi:10.1016/j.epsl.2015.08.026.

Manuscript received 12 September 2016
Revised manuscript received 25 November 2016
Manuscript accepted 1 December 2016

Printed in USA